# BARE MOLECULAR ANIONS OF UNSATURATED HYDROCARBONS: DENSITY FUNCTIONAL CHARGE AND SPIN DISTRIBUTIONS BASED ON THEIR SINGLE CRYSTAL STRUCTURES

Zdenek HAVLAS[a] and Hans BOCK[b]

[a] *Institute of Organic Chemistry and Biochemistry Academy of Sciences of the Czech Republic, 116 10 Prague 6, Czech Republic; e-mail: havlas@uochb.cas.cz*

[b] *Chemistry Department, University of Frankfurt, Marie-Curie-Str. 11, D-60439 Frankfurt/Main, Germany; e-mail: bock@risc.anorg.chemie.uni-frankfurt.de*

Received June 30, 1998
Accepted July 13, 1998

*Dedicated to our respected friend, Rudolf Zahradnik, on the occasion of his 70th birthday.*

Bare π-hydrocarbon radical anions $M^{\bullet\ominus}$, dianions $M^{\ominus\ominus}$ as well as even a radical trianion $M^{\bullet\ominus\ominus\ominus}$ can be crystallized as alkali metal salts, $[M^{(\bullet)\ominus n}]\ [Me^{\oplus}_{solv}]_n$ if the solvent-shared contact ion multiples, $[M^{(\bullet)\ominus n}\cdots(Me^{\oplus})_n]_{solv}$, present in aprotic solution after the reduction at an alkali metal mirror can be separated by advantageous cation solvation. Altogether 22 π-hydrocarbon anions $M^{(\bullet)\ominus n}$ comprising polycyclic *cata*- as well as *peri*-annelated six-membered ring compounds, polyphenyls, those with nonalternant polycyclic skeletal topology, open chain and organosilicon derivatives have been characterized by low-temperature X-ray crystallographic analyses. Based on the structural data determined, their charge and spin populations have been approximated by density functional calculations including natural bond orbital analyses (DFT/NBO). Although in general the total (σ + π) charges at individual C centers of the hydrocarbon skeletons cannot be correlated neither with the structural data nor with the spin distribution, numerous interesting details as well as some useful rules are provided. They concern, for instance, central C–C bond elongation and peripheral C–C bond shortening, preferred charge localization patterns, effects of conformational changes in the π-radical anions crystallized or Jahn–Teller distortions of formally degenerate molecular radical anion states.

**Key words:** Hydrocarbon radical anions; Radical ions; Density functional theory; X-Ray diffraction; *Ab initio* calculations.

Crystallization under aprotic conditions ($c_{H^{\oplus}}$ < 0.1 ppm) and in inert gas atmosphere demands skilled coworker craftmanship, the more if out a network of equilibria for the individual steps along a microscopic pathway in solution comprising electron transfer, cation solvation, contact ion formation or aggregation, a specific molecular ion salt is wanted for single crystal determination. For illustration of the "state of the art" reached after tedious optimization especially of "low gradient methods", the first contact ion quintuple of a π-hydrocarbon tetraanion[1] shall visualize exemplarily most of these aspects (Fig. 1).

Obviously, the tremendous structural changes observed such as the double-folding of the tetracene skeleton at the phenyl substitution centers up or down by 43° (!), rise the question to what extent each the $Na^{\oplus}$ countercation sandwich complexation between each two six-membered benzene rings and the charge distribution will contribute to the skeletal distortion of the hydrocarbon?

Countercation solvation plays an essential role in determining the formation of solvent-shared $[M^{\ominus n} Me^{\oplus}_{solv}]$ or solvent-separated $[M^{\ominus n}][Me^{\oplus}_{solv}]$ contact ion pairs[2]. Quite often their estimated crystal lattice sublimation enthalpies are approximately comparable. For an impressing and quite transparent example, the crystallization of both in the very same crystal is selected[3]: Tetraphenylbutadiene disodium forms within an equilibrium network in aprotic DME solution the solvent-shared $[M^{\ominus\ominus}(Na^{\oplus}DME_2)_2]$ as well as the solvent-separated contact ion triple $[M^{\ominus\ominus}][Na^{\oplus}DME_3]_2$, which due to optimum lattice packing crystallize together in the stoichiometric ratio 1 : 1 (Fig. 2).

In cutting an intricate story short[4], at least a third prototype possibility has to be emphasized: the crystallization of bare molecular anions $[M^{\bullet\ominus}]$ or $[M^{\ominus\ominus}]$, which can be experimentally achieved, if the solvated countercations are completely lipophilically shielded by full coordination to especially advantageous polyether or polyamine ligands such as diglyme[2] or pentamethyldiethylene triamine. For an example, the smallest and, therefore, most reactive naphthalene radical anion is selected[5] (Fig. 3).

The three examples of contact ion multiple structures chosen (Figs 1–3) demonstrate that the Frankfurt Group with its skilled coworkers has mastered most of the experimental difficulties of "low gradient" crystallization under aprotic and anaerobic conditions[4]. In addition, solvation enthalpies of countercations by various and especially polyether ligands used as suitable solvents have been quantum chemically estimated[2]. In order to elucidate whether the possibly tremendous structural changes observed after up to fourfold reduction (Fig. 1) of π-hydrocarbons[4] are predominantly caused by contact ion multiple formation or whether also the negative charge inflicted

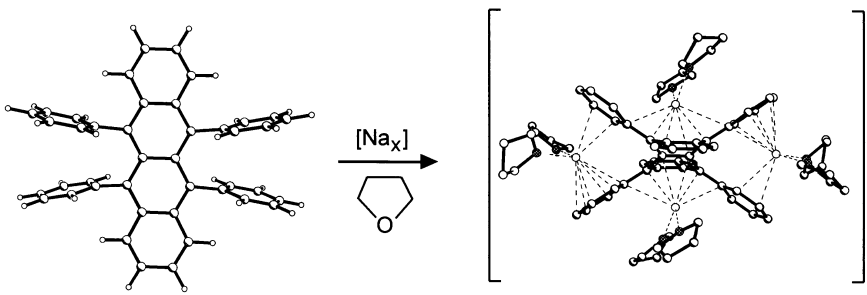


FIG. 1
Structural changes on the fourfold reduction of rubrene in aprotic THF solution and under argon at a sodium metal mirror to a contact-ion quintuple of its tetraanion, $[Rubrene^{\ominus\ominus\ominus\ominus}(Na^{\oplus}(THF)_2)_4]$

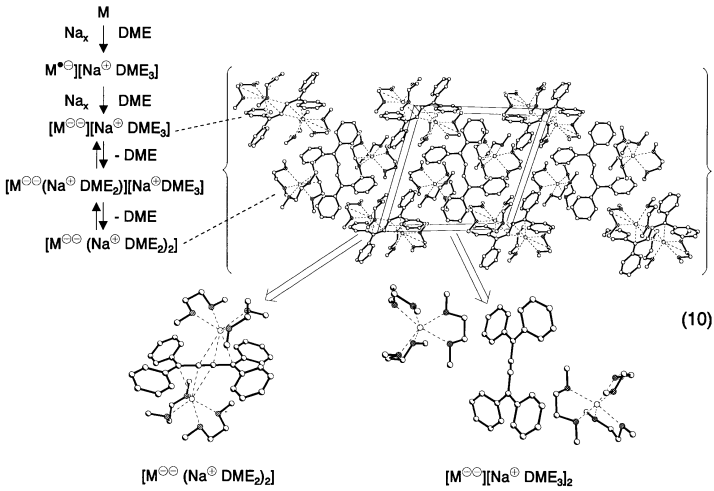


FIG. 2

Tetraphenylbutadiene reduction in aprotic DME solution at a sodium metal mirror to its dianion, which within an equilibrium network, forms both the solvent-shared and the solvent-separated contact triple ions, $[M^{\ominus\ominus}][Na^{\oplus}DME_2]_2$ and $[M^{\ominus\ominus}][Na^{\oplus}DME_3]_2$

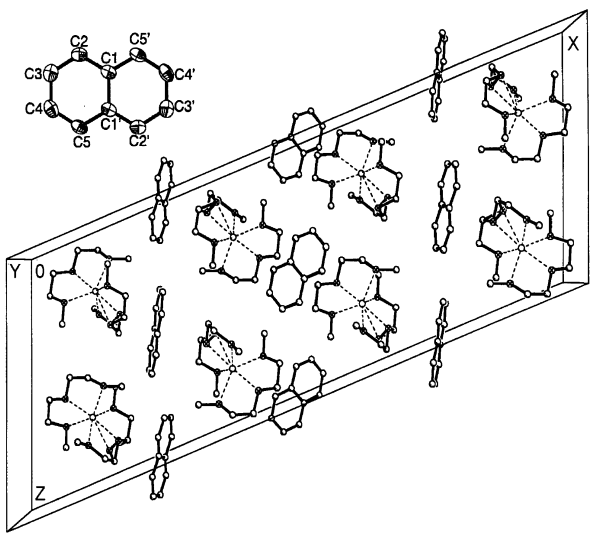


FIG. 3

Structure of naphthalene–bis(diglyme)sodium in its black single crystal, grown from an aprotic diglyme solution after reduction of the π-hydrocarbon at a sodium mirror in an argon atmosphere

on the carbon skeleton plays some role, we have crystallized by design more than 20 solvent-separated salts containing "bare" molecular radical anions, dianions as well as trianions, which may be classified as proposed in Scheme 1, and determined their structures[4,6].

Here we report on charge and spin populations of the bare radical anions and dianions obtained from natural bond orbital (NBO) analysis of density functional theory (DFT) calculations based on the experimentally determined structural data[6].

## COMPUTATIONS

The DFT calculations have been performed based on the structural data using Becke's three-parameter functional[7], VWN correlation functional[8], and LYP nonlocal correlation[9], know as B3LYP hybrid functional. The calculation of the wave functions was followed by NBO analysis[10]. A basis set of VDZ+P quality (6-31G*) has been employed for all molecules. The open-shell systems were computed using the unrestricted formalism (UB3LYP). The resulting charges and spin densities are plotted with home-made routines, which utilize the post-script output of the XMOL program.

In all figures the α-spin is defined to be positive. For plotting of atomic charges, "group" charges including hydrogen bonded to the respective center were preferred to avoid the usually large C–H bond polarity predicted by any population analysis. The computations were performed using the GAUSSIAN94 program[11] on SGI Octane and NEC SX4 computers.

## RESULTS AND DISCUSSION

The combined efforts to crystallize of extremely air-sensitive salts of bare hydrocarbon anions, determination of their low temperature structures, and to approximate by DFT/NBO calculations their charge and spin populations are directed towards information on the extent of structural distortions (Figs 1–3) by negative charges, on the charge distribution over topologically different hydrocarbon skeletons as well as on correlation between charge and spin at individual centers of the π-systems.

Even for a more qualitative discussion, assumptions have to be made concerning, for instance, potential polarization effects of the solvent-separated and lipophilically wrapped countercations on the hydrocarbon anions[12]. To tackle this problem on an experimental basis, each the shortest distance between the centroid of the respective π-hydrocarbon anion [$M^{\ominus n}$] and the solvent-separated [$Me^{\oplus}_{solv}$] or solvent-shared [$M^{\bullet\ominus n}\cdots Me^{\oplus}_{solv}$] countercation in selected representative salts (Scheme 1: X), has been extracted from the structural data sets (Table I).

The largest distance differences are observed between the solvent-shared contact ion multiples (1 : C in Table I) and the solvent separated ones: The solvent shell around the countercation at least doubles the distances $M^{\ominus n}\cdots Me^{\oplus}$ (ref.[2]) depending on the size of

▷ Polycyclic (Six-Membered Ring) Hydrocarbons: Acenes

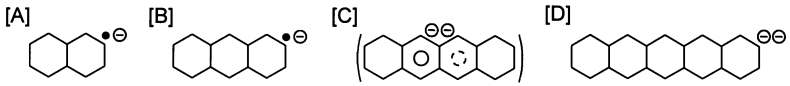


▷ Acene Derivatives and Isomers

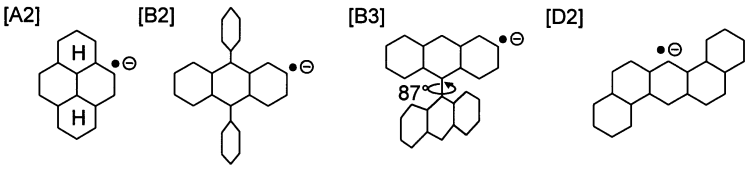


▷ Linear and Cyclic Polyphenyls

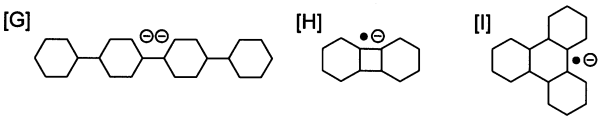


▷ Nonalternant Polycyclic Hydrocarbons

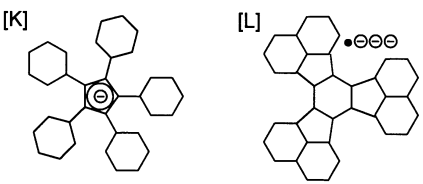


▷ Open-Chain π-Hydrocarbons

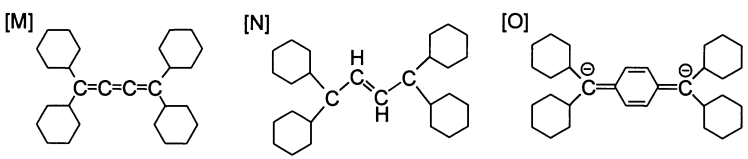


▷ Organosilicon Derivatives of Cyclic Hydrocarbons

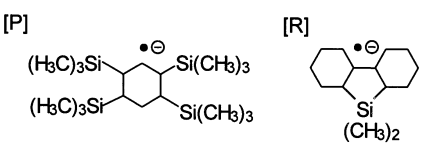


SCHEME 1

Topology of π-hydrocarbon anions investigated. Brackets mean solvent-shared contact ion multiple

both the cation ($Me^{\oplus}$) (1 : F in Table I), and especially on inclusion of its solvent shell ($Me^{\oplus}_{solv}$ ) (1 : B2 in Table I). Steric overcrowding in the hydrocarbon anions (1 : P in Table I) or substituent twisting out of the molecular plane, which hampers stapling within the crystal (1 : B2 in Table I), also play some role. The range of the shortest distances $[M^{\ominus n}]\cdots[Me^{\oplus}_{solv}]$ of about 500 to 800 pm (Table I) indicates only weak Coulomb interactions. Specific polarization effects by an individual cation $Me^{\oplus}_{solv}$ on the electron distribution within the π-hydrocarbon anion are assumed to be rather unlikely because in general several $Me^{\oplus}$ surround each $M^{\ominus n}$ in the crystal, providing an approximately isotropic Coulomb field.

Severe structural changes are usually observed only in solvent-shared contact ion multiples such as the rubrene tetraanion contact ion quintuple (Fig. 1). In solvent-separated radical anions salts, the distortion of the hydrocarbon skeleton is frequently almost negligible, whereas in bare dianions often significant bond length and angle changes are detected. In contrast, deviations from planarity, if observed at all, are usually found to be only small. For illustration, the charge-inflicted-structural perturbations of the naphthalene radical anion (A) and pentacene dianion (B) are presented (Scheme 2).

Summarizing the preliminary remarks concerning cation polarization effects on the charge distribution in solvent-separated "bare" hydrocarbon anions, their neglect seems to be justified. Smaller structural distortions of neutral hydrocarbons on insertion of one or two electrons usually do not require special efforts *e.g.* by hypersurface calculations.

TABLE I

Distances between the centroid of the π-hydrocarbon anion and the countercation in selected solvent-shared and solvent-separated ion aggregates

| Class from Scheme 1 (1: X) | Selected example | Distance $M^{\bullet\ominus}\cdots M^{\oplus}$ pm |
|---|---|---|
| | Solvent-shared | |
| (1: C) | $[Tetracene^{\ominus\ominus}]\cdots[(K^{\oplus}Triglyme)_2]$ | 275 |
| | Solvent-separated | |
| (1: A) | $[Naphthalene^{\bullet\ominus}]\cdots[Na^{\oplus}(Diglyme)_2]$ | 568 |
| (1: F) | $[Perylene^{\bullet\ominus}]\cdots[Na^{\oplus}(Diglyme)_2]$ | 572 |
| | $[Perylene^{\bullet\ominus}]\cdots[Cs^{\oplus}(Tetraglyme)_2]$ | |
| (1: D) | $[Pentacene^{\ominus\ominus}]\cdots[Na^{\oplus}(DME)_3]_2$ | 634 |
| (1: P) | $[2,3,5,6\text{-Tetrakis(trimethylsilyl)benzene}^{\ominus\ominus}]\cdots[Na^{\oplus}(DME)_3]_2$ | 649 |
| (1: B2) | $[9,10\text{-Diphenylanthracene}^{\bullet\ominus}]\cdots[Na^{\oplus}(THF)_6]$ | 728 |

In conclusion it is pointed out again that all DFT/NBO computations have been performed starting from the experimentally determined low-temperature structures. The report on charge and spin populations in bare π-hydrocarbon radical anions and dianions will follow the outline forwarded (Scheme 1).

*Polycyclic (Six-Membered Ring) Hydrocarbons: Acenes*

Crystal growth of three compounds has been achieved, which all contain bare anionic species: Naphthalene radical anion (Scheme 1: A), anthracene radical anion (Scheme 1: B) and pentacene dianion (Scheme 1: D). For comparison also the contact ion triple [tetracene$^{\ominus\ominus}$($K^{\oplus}$diglyme)$_2$] (Scheme 1: C) is presented. Characteristic structural data[6,13] and the results of the DFT/NBO analysis of charge and spin populations are schematically summarized for comparison in Fig. 4.

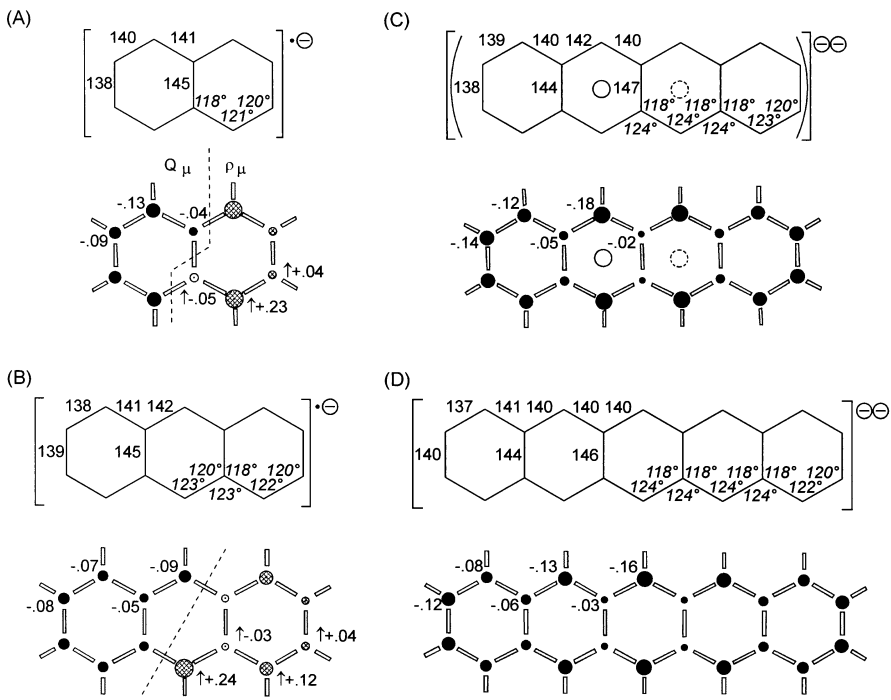


FIG. 4

Representative examples of two "bare" acene radical anions (A, B) and one dianion (D), as well as for comparison of a solvent-shared dianion (C: ❍ and ❍ $Me^{\oplus}$ positions above and below the hydrocarbon plane): Essential structural data (left-hand side: bond lengths in pm; right-hand side: angles) together with DFT/NBO charge (left-hand side) and spin (right-hand side) populations (see text)

On one-electron reduction of naphthalene or anthracene in diglyme solution at a sodium mirror their solvent-separated radical anion salts $[M^{\bullet\ominus}][Na^{\oplus}(diglyme)_2]$ crystallize[13], in which the central C–C bonds are lengthened and the peripheral ones are shortened by several pm (Scheme 2 and Figs 4A and 4B). Simultaneously, the angles along the carbon ribbons are widened by up to 3°. The charge distributions calculated for the naphthalene radical anion are largest in 1, 4, 5, 8 positions and smallest at the central C–C bond centers and therefore, hardly can be correlated with the structural data. The spin is also preferentially located at the 1, 4, 5, 8 carbon centers in the naphthalene and at the 9, 10 centers in anthracene radical anion. In the dianions, solvent-shared in the tetracene and solvent-separated in the pentacene salts[6] $[tetracene^{\ominus\ominus}(K^{\oplus}triglyme)_2]$ and $[pentacene^{\ominus\ominus}][Na^{\oplus}(DME)_3]_2$, again the charge populations at the peripheral C centers dominate. In contrast to the almost planar pentacene dianion, the skeleton of the solvent-shared tetracene contact ion triple (Fig. 4C: ❍/❍ countercations above and below the molecular plane), the hydrocarbon is bent twice in opposite directions by about 8° (*cf.* Fig. 1) – a small but significant structural difference between both chemically related, but differently solvated dianion salts.

*Acene Derivatives and Isomers*

For further discussion of acene radical anions (Fig. 4), alkali salts of the singly reduced hydrocarbons 1,2,3,6,7,8-hexahydropyrene, 9,10-diphenylanthracene, 1,1′-bianthryl, 1,2,5,6-dibenzanthracene, phenanthrene and perylene are presented with their essential structural data as well as DFT/NBO charge and spin populations in Fig. 5.

The results (Fig. 5) are commented on as follows: The hexahydropyrene radical anion expectedly resembles the one of naphthalene (Fig. 4A) with its peripheral bonds shortened contrary to the central bond, which exhibits again small charge and spin populations (Fig. 5A). In 9,10-diphenylanthracene radical anion the phenyl rings are twisted by 67° (ref.[13]), corresponding to a considerably reduced π-interaction of only $\beta = \beta_0(\cos^2 \omega) = 0.15\ \beta_0$, and, therefore, a close analogy to the radical anion of unsubstituted anthracene is expected and observed. On the contrary, in 1,1′-bianthryl radical anion with close to perpendicular π-components[13] (Fig. 5C, ω = 87°, connecting C–C bond 144 pm) both the charge and the spin populations, calculated and based on the

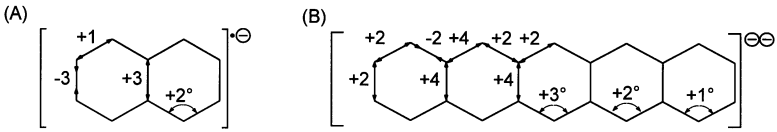


SCHEME 2
Charge perturbation of bond lengths (pm) and angles in selected π-hydrocarbons on single and two-fold electron insertion

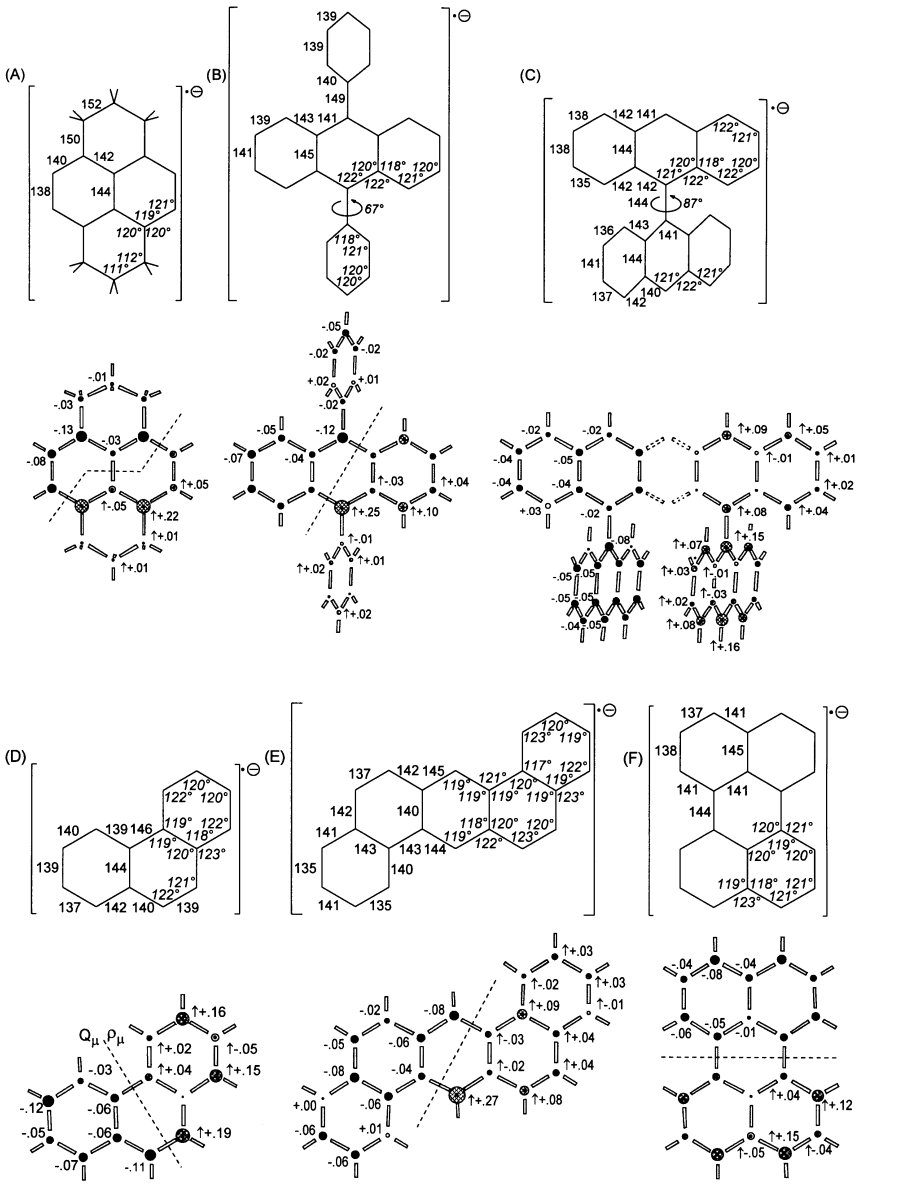


FIG. 5

Bare radical anions of acene derivatives (A, B, C) and differently benz-annelated isomers (D, E, F) in their solvent-separated alkali salts: Essential structural data (each above) and DFT/NBO charge $Q_\mu$ as well as $M^{\bullet\ominus}$ spin $\rho_\mu$ populations (see text)

structural data, differ considerably and suggest that the extra electron is preferentially located in one molecular half. A comparison of the isomeric anthracene and phenanthrene radical anions (Figs 4B and 5D) reveals interesting information. In contrast to anthracene (Scheme 2), the structure of phenanthrene[14] remains nearly unchanged on electron insertion. Only the peripheral C–C bond of the middle ring stretches by 4 to 139 pm (Fig. 5D) and for its C centers as well as for those in the respective *para*-positions, the largest charge and spin populations are calculated. On continued comparison between 1,2,5,6-dibenzanthracene (Fig. 5E) and anthracene (Fig. 4B) radical anions, the ring-connecting C–C bonds suggest an replacement of the outer $C_6$ rings by naphthalene subunits: the former C(11)–C(12) bond shortens from 145 to 140 pm and the C(5)–C(6) one stretches from 138 to 143 pm. However, the "biphenyl-type" C–C bond is 143 pm long and the opposite one 137 pm short (Fig. 5D, phenanthrene $^{\bullet\ominus}$ 146 and 139 pm) and the highest spin populations are calculated again for the "central anthracene" positions 9 and 10. Attempts to grow crystals of isomeric dibenzanthracene radical anions are under way to obtain further information on the interesting benzannelation effects. As concluding example, perylene radical anion (Fig. 5E) is presented: Again electron insertion elongates the ring-connecting bonds[14] by 2 pm and shortens the C–C distances between the "naphthalene-type" subunits[14] by 3 pm. The largest change and spin populations are calculated at centers 1, 3, 4, 6, 7, 9, 10, and 12, *i.e.* for the peripheral C centers adjacent to threefold coordinated ones.

*Linear and Cyclic Polyphenyls*

In addition to *cata*- (Figs 4 and 5) and *peri*-condensed (Fig. 5E) polyarenes[14], also chain-linked polyphenyls are composed exclusively out of six-membered, "unsaturated" rings. The linear ones show considerable flexibility around their ring-connecting C–C bonds, the rotational barriers of which increase rapidly with the volume of *ortho*-substituents[14]. So far, single crystals could been grown and structures determined of quarterphenyl dianion (Fig. 6A) and of biphenylene (Fig. 6B) as well as triphenylene (Fig. 6C) radical anions[6].

In the quarterphenyl dianion (Fig. 6A) the following structural differences are observed relative to neutral biphenyl (which is twisted around its central C–C bond by 42° in the gas phase, but planar in the single crystal[15,16]): The untwisted $M^{\ominus\ominus}$ is slightly bent twice by about 8° along the intramolecular long axis in S-shape conformation with the phenyl-CC-connections shortened by 7 to 9 pm, a surprisingly large charge perturbation. Within the phenyl rings, the ipso angles shrink by about 2 to 113° and C–C bond lengths alternate between 136 and 142 pm relative to the smaller alternation between 138 and 140 pm in the crystalline biphenyl with analogously planar phenyl rings. The largest charge populations are calculated for the C centers along the intramolecular long axis and, surprisingly, they alternate. In the biphenylene and triphenylene radical anions (Figs 6B and 6C) no significant bond length and angle changes are observed

relative to the uncharged molecules[14] including the central ring bond alternation in the triphenylene radical anion (Fig. 6C).

The DFT/NBO total charge and spin populations for the two radical anions (Figs 6B and 6C) require special comments. Whereas the almost coinciding $Q_\mu/\rho_\mu$ patterns for the biphenyl derivative can be rationalized even by qualitative MO wavefunctions squared[17], the two degenerate radical anion states of $D_{3h}$-symmetric triphenylene should cause a Jahn–Teller distortion. Although barely reflected in the structural data within their experimental accuracy, the calculations predict the charge population of the lowest radical anion state to slightly dominate only in two of the three six-membered rings (Fig. 6C, --- plane of symmetry). Expectedly, the spin population is perturbed

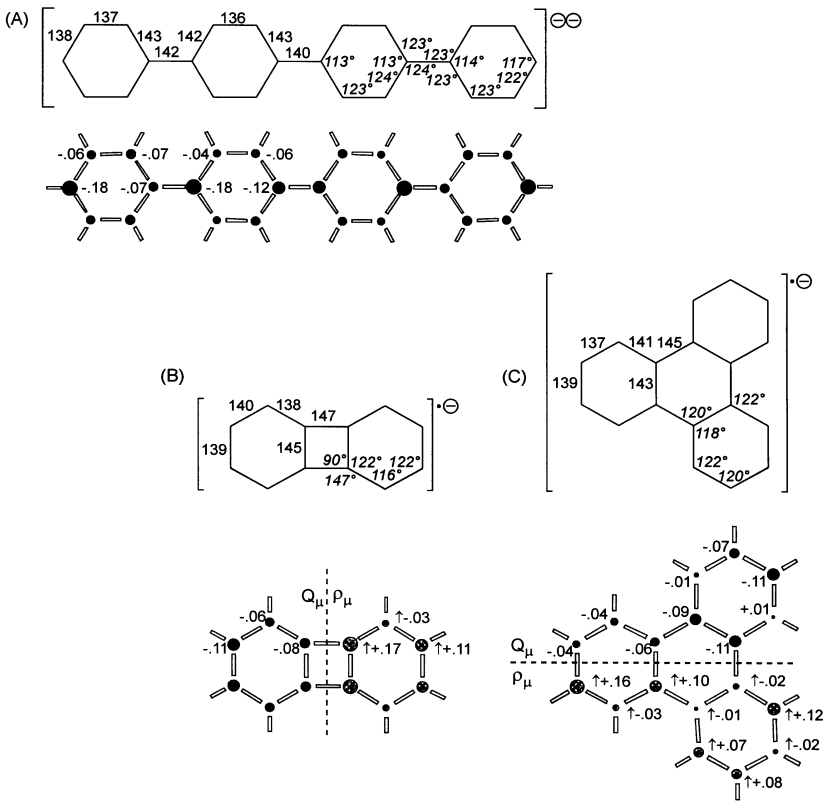


FIG. 6

Bare quarterphenyl dianion (A) and biphenylene as well as triphenylene radical anions (B, C) in their solvent-separated alkali salts: Essential structural data (each above) and DFT/NBO charge $Q_\mu$ as well as $M^{\bullet\ominus}$ spin populations $\rho_\mu$ (each below; see text)

considerably stronger. The largest differences between charge and spin populations have been calculated so far for the triplet biradical tris(3,5-di(*tert*-butyl)-4-oxophenylene)methane also containing three six-membered quinoid-distorted rings around a threefold axis ($D_{3h}$), which could be grown in violet single crystals and structurally characterized[18].

*Nonalternant Polycyclic Hydrocarbons*

The fascinating topological phenomenon of alternancy[17] is transparently demonstrated in π-hydrocarbon radical anions and cations[19,20]. Therefore, both the non-alternant radical trianion of decacyclene (Scheme 1: L) and the radical anion of pentaphenylcyclopentadiene (Scheme 1: K) have been crystallized as solvent-separated alkali salts and their structures determined[6] (Figs 7A and 7B).

Due to its threefold rotational axis, the radical trianion of decacyclene (Fig. 7A) should Jahn–Teller distort as already discussed for the triphenylene radical anion (Fig. 6C).

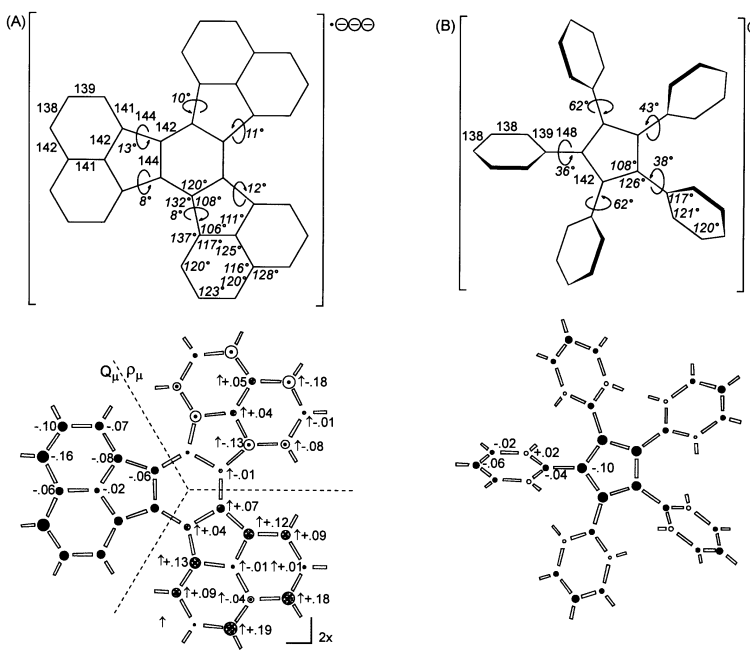


FIG. 7

Bare decacyclene radical trianion (A) and pentaphenyl cyclopentadienyl anion (B) in their solvent-separated alkali salts: Essential structural data (left-hand side: bond lengths (pm), right-hand side: angles) and DFT/NBO charge $Q_\mu$ and $M^{\bullet\ominus\ominus\ominus}$ spin populations $\rho_\mu$

Again, the Jahn–Teller distortion of the skeletal structure is presumably too small to be assigned within the usual accuracy limits (±1 pm, ±1°) of the 180 K structure determinations (*cf.* triphenylene[6]: $R_1$ = 0.041, $R_2$ = 0.093), which reveals the drastic changes due to the three negative charges: The acenaphthalene subunits are twisted out of the molecular plane expected for the neutral hydrocarbon by dihedral angles between 8 and 12°. In the resulting propeller-shaped conformation, some charge localization within the five-membered rings is indicated by the cyclopentadienyl anion-like equilibration of the C–C bond lengths (Fig. 7B), whereas the central C–C bond in the naphthalene fragment is 4 pm shorter than in the bare naphthalene radical anion (Fig. 4A). Again (*cf.* Fig. 6C) the calculated DFT/NBO populations differ considerably: Contrary to the rather even charge distribution around an approximate $C_3$ axis through the center of the trianion, the spin is arranged according to a plane of symmetry with two substituent units exhibiting each a large positive population and the third propeller-blade a smaller negative one.

The pentaphenyl substituted cyclopentadienyl anion shows the expected structure (Fig. 7B) with equal C–C bond lengths and ipso angles. The phenyl rings with standard bond lengths and angles[21] are arranged in an interesting conformational pattern to avoid a possibly repulsive van der Waals interaction between their *ortho*-hydrogens: Two in 1,3-positions with dihedral angles of each 62° enforce a 36° twisting of the one in 2-position, whereas the 4- and 5-substituents are turned 38 and 43°, respectively. The DFT/NBO charge population calculated from the structural data confirms that the about half of the charge is delocalized within the five-membered ring and about one tenth only in each phenyl substituent.

### *Open-Chain π-Hydrocarbons: Tetraphenyl Substituted Dianions*

The concept of crystallizing π-hydrocarbon salts with bare molecular anions by solvent-separation of the countercations can be extended to unsaturated carbon chains, at least if some charge delocalization *e.g.* in to phenyl substituents helps to stabilize the rather reactive species to persistent compounds. Crystals containing bare dianions could be grown after sodium metal mirror reduction of π-hydrocarbons or after deprotonation of hydrogen-richer ones and low-temperature structures determined[4,6] (Fig. 8) for the bare dianions of tetraphenylbutatriene, 1,1,4,4-tetraphenylbutadiene and 7,7,8,8-tetraphenyl-*p*-xylene.

All dianion structures (Fig. 8) are published[3,4,22,23] and, therefore, only some essential structural features as well as the hitherto unknown DFT/NBO charge populations will be discussed. To begin with tetraphenylbutatriene, the neutral molecule is close to planar[22] and its C=C bond lengths vary between 135 and 126 pm, exceeded by the differences of 139 and 124 pm in the also structurally characterized radical anion[22]. The dianion exhibits even stronger distortions: The bond lengths changes reach a breathtaking size between 143 pm for the outer and 123 pm for the central C–C bond.

Accordingly, an acetylene dianion is formed, the $(H_5C_6)_2C^{\ominus}$ halves of which are twisted almost perpendicular to each other by severe cyanine perturbation[4]. The charge population calculated corroborates the structural findings: The C centers at the end of the chain are rather anionic in character, despite of charge delocalization in the adjacent phenyl rings (Fig. 8A).

For the bare tetraphenylbutadiene dianion, which cocrystallizes with its solvent-shared contact ion triple (Fig. 2), analogous structural changes are observed: On two-electron reduction, the C–C bond lengths are reversed from C(1)=C(2) with 136 pm and C(2)–C(3) with 144 pm to C(1)–C(2) with 146 pm and C(2)–C(3) with 138 pm (refs[3,4]).

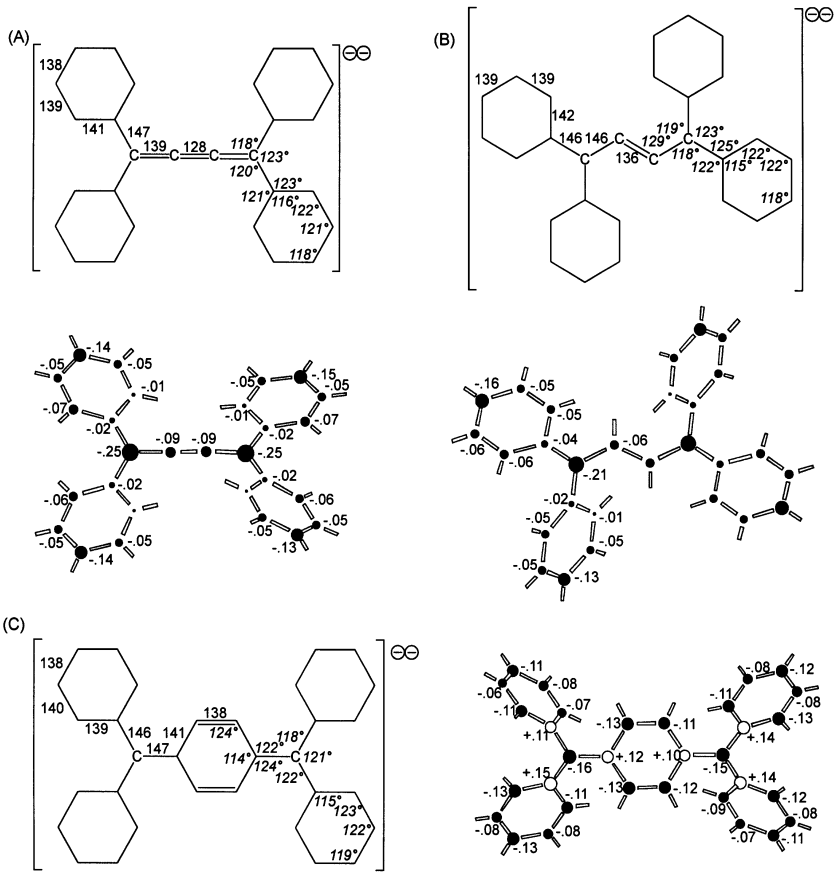


FIG. 8

Bare dianions of tetraphenylbutatriene (A), 1,1,4,4-tetraphenylbutadiene (B) and 7,7,8,8-tetraphenyl-*p*-xylene (C) in their solvent-separated sodium salts: Essential structural data (left-hand side bond lengths (pm), right-hand side angles) and DFT/NBO charge distributions (see text)

For the planar dianion skeleton again heavy negative charges at both chain end C centers are calculated with some delocalization especially to the phenyl *para*-positions.

Tetraphenyl-*p*-quinodimethane dianion[23] exhibits different, but also severe bond lengths changes relative to the neutral molecule: the outer C(1)=C(2) bond is elongated by 9 pm (!) on two-electron insertion to 147 pm and the phenyl ring C–C bonds are shortened by 4 to 141 pm or stretched by 3 to 138 pm. The dianion structure (Fig. 8C), therefore, corresponds rather to a twofold $(H_5C_6)_2C^{\ominus}$-substituted phenyl ring derivative, for which a difficult to rationalize, highly polarized carbon skeleton with intermittent positive centers is predicted by the DFT/NBO calculations.

*Organosilicon Derivates of Cyclic Hydrocarbons*

In closing, the manifold of bare π-hydrocarbon anions $M^{(\bullet)\ominus n}$ presented is extended by two selected examples of compounds containing Si hetero substituents, the element closest to carbon in the periodic table, but differing tremendously in its much lower effective nuclear charge[23]: Accordingly, $R_nSi$ groups are powerful donors in β-position to π-systems *i.e.* in $R_3SiCH_2$ substituents, whereas in α-position they act as effective acceptors[23,24]. For illustration of the two different perturbations within and outside of π-systems each one bare radical anion is chosen, *i.e.* the ones of 1,2,4,5-tetrakis(trimethylsilyl)benzene[26] (Fig. 9A) and of 9,9-dimethylsilafluorene[27] (Fig. 9B).

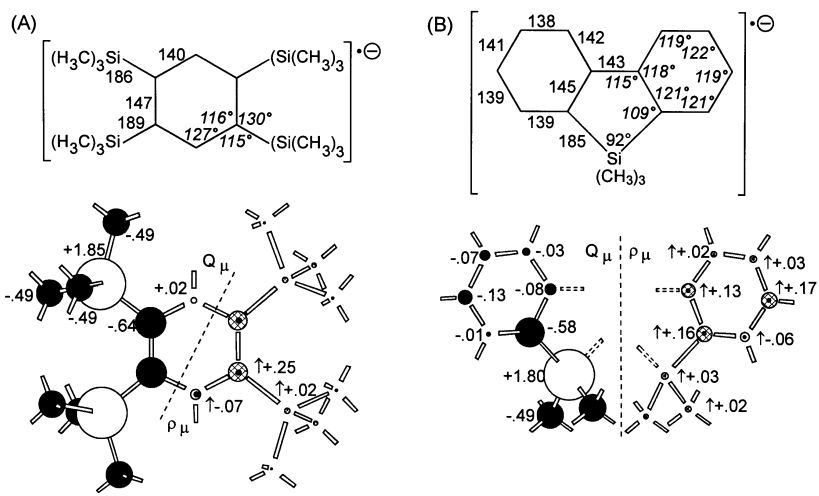


FIG. 9

Bare radical anions of 1,2,4,5-tetrakis(trimethylsilyl)benzene (A) and 9,9-dimethylsila-fluorene (B) in their solvent-separated sodium salts: Essential structural data (each above, bond lengths in pm) and DFT/NBO charge $Q_\mu$ as well as spin $\rho_\mu$ populations (see text)

The structure of the tetrakis(trimethylsilyl)benzene radical anion reveals an almost unbelievable distortion relative to neutral molecule: The ring CC bonds between each the $R_3Si$ substitution centers is elongated from 141 pm by 6 pm to 147 pm (ref.[26]), indicating a severe cyanine distortion[4] presumably due to the delocalization of negative charge along the two chain fragments $(Si{=}C{=}C{=}C{=}Si)^{\delta\ominus}$ (ref.[26]). The DFT/NBO total charge distributions confirm this assumption (Fig. 8A): The dominating positive charge at the silicon centers is expected from the difference C/Si in their first atomic ionization potentials of about 3 eV (!) (ref.[24]) and largely compensated by the surrounding methyl carbons. The C substitution centers in the ring are predicted to carry a relatively large negative charge, which correlates with a repulsive elongation of the connecting C–C bond and which despite the nodal symmetry plane through the long axis should be delocalized around the ring as is confirmed by ESR experiment[26].

The radical anion of 9,9-dimethylsilafluorene is generated by ($R_2Si$) insertion into biphenylene radical anion (Fig. 6B, ref.[27]) and the $Na^{\oplus}$ countercation is separated by 2.2.1.-cryptand encapsulation. The low-temperature structure determination reveals planar five- and six-membered rings and, in general, standard geometries[21], except for 4 pm changes in the lengths of the five-membered ring C–C bonds and the rather small angle ∢ CSiC of only 92°. The skeleton of the radical anion is, therefore, at best only slightly distorted and the DFT/NBO results should illustrate the electronic effect in organosilicon anions more reliably than on the background noise of a severe cyanine distortion (Fig. 6A). Again a large positive charge for the Si center is expectedly predicted, partly compensated by the surrounding carbons. Due to the larger radical anion π-system, the largest negative charge at the adjacent ring C centers is smaller than in the benzene radical anion (Fig. 9A). The net charges $\Sigma_\mu Q_\mu$ in the central rings amount to –0.25 ($C_6$) *vs* –0.05 ($C_4Si$), suggesting that the stabilization of radical anions by Si centers due to their low effective nuclear charge might be more pronounced inside a π-system than on outside substitution.

## RETROSPECT AND PERSPECTIVE

The improved techniques of low gradient crystallization made possible to grow crystals of solvent-separated alkali salts containing bare anions of hydrocarbons. Based on their structural data, density functional calculations including natural bond orbital analyses have been performed, which yield both total (σ + π) charge and, for dublet states, also spin distributions.

Altogether 22 hydrocarbon radical anions $M^{(\bullet)\ominus}$, dianions $M^{\ominus\ominus}$ and one radical trianion $M^{(\bullet)\ominus\ominus\ominus}$ are investigated comprising six-membered ring cata- and peri-condensed polycyclic compounds and polyphenyls as well as nonalternant, open-chain and organosilicon derivatives. One essential assumption, which concerns the neglect of potential polarization effects of the countercations on the hydrocarbon anions can be partially

justified by both the rather large distances between them and the cation arrangement around the anions in the crystal.

The wealth of information obtained on comparison, correlation attempts and discussion based on perturbation arguments, provides – at least at first sight – the following results:

*a*) The DFT/NBO results, although based on experimental structural data, often do not correlate beyond doubt with the total ($\sigma + \pi$) charges calculated.

*b*) In contrast to the usually successful numerical assignment of ESR hydrogen signal patterns by squared HMO $\pi$ coefficients of the adjacent carbon $\pi$ centers *via e.g.* the McConnell relationship, $a^{\pi}_{\mu,X} = | Q_X | (c^{HMO}_{J\mu})^2$, the open-shell DFT/NBO spin populations do not always fit into such a generally applicable correlation.

*c*) Nevertheless, the DFT/NBO results on hydrocarbon anions provide many useful hints for the preparative chemist such as: In acene derivatives large charges are predicted at peripheral C centers connected by rather short C–C bonds, whereas small charges are calculated for the C centers at the elongated inter-ring ones. Conformational changes by twisting substituents around their connecting C–C bonds to the parent system can be reasonably rationalized as exemplified for 9,10-diphenylanthracene or 1,1′-bianthryl radical anions, including the seemingly surprising prediction of predominantly localized spin in one molecular half of the latter. In the $D_{3h}$-symmetric radical anion of triphenylene, the Jahn–Teller distortion of the degenerate states is satisfactorily reproduced. In radical anions of non-alternant hydrocarbons and in the dianions of tetraphenyl substituted linear and branched carbon chain compounds, each the characteristic facets revealed by their structure determinations are well covered by the DFT/NBO results. Last, but not least, the perturbations in organosilicon radical anions due to the low effective Si nuclear charge demonstrate – with the different effects of outside substitution and of internal C→Si replacement – the rewarding general applicability of combined crystallization and calculation efforts.

The main perspective for future work should be to experimentally determine the structure of the respective neutral hydrocarbon molecules, by either extensively searching the Cambridge Structural Database or, if necessary, by crystallization and X-ray analysis. In addition, their DFT/NBO charge distributions have to be calculated in order to compare the changes inflicted on the hydrocarbon skeletons by electron insertion. It also would be helpful to correlate the ESR/ENDOR coupling constants of their radical anions in solutions with the DFT/NBO spin populations reported.

*The authors gratefully acknowledge the support of their long-time cooperation by the Humboldt Foundation, the Academy of Sciences of the Czech Republic in Prague, the Hoechst Corporation as well as the Freunde und Forderer of the University in Frankfurt. We are also very grateful to Dipl.-Chem. V. Krenzel for help in the preparation of the manuscript including the figures. The Hochstleistungs-Rechenzentrum of the Technical University in Stuttgart and the Academy of Sciences in Prague provided time on their NEC SX4 computers.*

**REFERENCES**


1. a) Bock H., Gharagozloo-Hubmann K., Nather C., Nagel N., Havlas Z.: *Angew. Chem.* **1996**, *108*, 720; b) Bock H., Gharagozloo-Hubmann K., Nather C., Nagel N., Havlas Z.: *Angew. Chem., Int. Ed. Engl.* **1996**, *35*, 631.
2. a) Bock H., Nather C., Havlas Z., John A., Arad C.: *Angew. Chem.* **1994**, *106*, 1823; b) Bock H., Nather C., Havlas Z., John A., Arad C.: *Angew. Chem., Int. Ed. Engl.* **1994**, *33*, 1755; and references therein.
3. Bock H., Nather C., Ruppert K., Havlas Z.: *J. Am. Chem. Soc.* **1992**, *114*, 6907.
4. a) Bock H., Ruppert K., Nather C., Havlas Z., Herrmann H.-F., Arad C., Göbel I., John A., Meuret J., Nick S., Rauschenbach A., Seitz W., Vaupel T., Solouki B.: *Angew. Chem.* **1992**, *104*, 595; b) Bock H., Ruppert K., Nather C., Havlas Z., Herrmann H.-F., Arad C., Gobel I., John A., Meuret J., Nick S., Rauschenbach A., Seitz W., Vaupel T., Solouki B.: *Angew. Chem., Int. Ed. Engl.* **1992**, *31*, 550.
5. Bock H., Arad C., Nather C., Havlas Z.: *J. Chem. Soc., Chem. Commun.* **1995**, 2393.
6. All structures of compounds, for which no literature quotation is given in the text, are published in the *Ph.D. Theses* submitted at the Chemistry Department of the University Frankfurt (year in brackets): Nather C. (**1995**), Hauck T. (**1996**), Arad C. (**1997**), Sievert M. (**1997**), Gharagozloo-Hubmann K. (**1998**), Nagel N. (**1998**), and Holl S. (**1998**).
7. Becke A. D.: *J. Chem. Phys.* **1993**, *98*, 5648.
8. Wasko S. H., Wilk L., Nursiar M.: *Can. J. Phys.* **1980**, *58*, 1200.
9. a) Lee C. Yang, W. Parr R. G.: *Phys. Rev. B: Condens. Matter* **1988**, *37*, 785; b) Miehlich B., Sarin A., Stoll H., Preuss H.: *Chem. Phys. Lett.* **1989**, *157*, 200.
10. Read A. E., Curtiss L. A., Weinhold F.: *Chem. Rev.* **1998**, *88*, 899.
11. Frisch M. J., Trucks G. W., Schlegel H. B., Gill P. M. W., Johnson B. G., Robb M. A., Cheeseman J. R., Keith T., Petersson G. A., Montgomery J. A., Raghavachari K., Al-Laham M. A., Zekrzewski V. G., Ortiz J. V., Foresman J. B., Cioslowski J., Stafanov B. B., Nanayakkara A., Challacombe M., Peng C. Y., Ayala P. Y., Chen W., Wong M. W., Andres J. L., Replogle E. S., Gomperts R., Martin R. L., Fox D. J., Binkley J. S., Defrees D. J., Baker J., Stewart J. P., Head-Gordon M., Gonzales C., Pople J. A.: *GAUSSIAN94, Revision E.2*. Gaussian Inc., Pittsburgh, PA 1995.
12. *Cf. e.g.* Kremer T., Schleyer P. v. R.: *Organometallics* **1997**, *16*, 737; and references therein.
13. a) Bock H., John A., Nather C., Havlas Z., Mihokova E.: *Helv. Chim. Acta* **1994**, *77*, 41; b) Bock H., John A., Nather C., Havlas Z.: *Z. Naturforsch. B: Chem. Sci.* **1994**, *49*, 1339.
14. Harvey R. G.: *Polycyclic Aromatic Hydrocarbons*. Wiley-VCH, New York 1997.
15. Bock H., Sievert M., Havlas Z.: *Chem. Eur. J.* **1998**, *5*, 677; and references therein.
16. Bock H., Nick S., Nather C., Bensch W.: *Chem. Eur. J.* **1995**, *1*, 557; and references therein.
17. *Cf. e.g.* Heilbronner E., Bock H.: *The HMO Model and Its Application*. Wiley, London 1976.
18. a) Bock H., John A., Havlas Z., Bats J. W.: *Angew. Chem.* **1993**, *105*, 416; b) Bock H., John A., Havlas Z., Bats J. W.: *Angew. Chem., Int. Ed. Engl.* **1993**, *32*, 416.
19. a) Bock H.: *Angew. Chem.* **1977**, *89*, 631; b) Bock H.: *Angew. Chem., Int. Ed. Engl.* **1977**, *16*, 613; and references therein.
20. Bock H., Rohn G.: *Helv. Chim. Acta* **1991**, *74*, 1221.
21. Burgi H.-B., Dunitz J. D. (Eds): *Structure Correlation*, Appendix A. VCH, Weinheim 1994.
22. Bock H., Arad C., Gobel I., John A., Baur R.: *Z. Naturforsch. B: Chem. Sci.* **1996**, *51*, 1381.
23. Bock H., Arad C., Gobel I., John A.: *Z. Naturforsch. B: Chem. Sci.* **1996**, *51*, 1391.
24. a) Bock H.: *Angew. Chem.* **1989**, *101*, 1659; b) Bock H.: *Angew. Chem., Int. Ed. Engl.* **1989**, *28*, 1627.

25. a) Bock H., Meuret J., Ruppert K.: *Angew. Chem.* **1993**, *105*, 413; b) Bock H., Meuret J., Ruppert K.: *Angew. Chem., Int. Ed. Engl.* **1993**, *32*, 414.
26. Bock H., Ansari M., Nagel N., Havlas Z.: *J. Organomet. Chem.* **1995**, *63*, 499.
27. Bock H., Sievert. M., Bogdan C. L., Kolbesen B. O., Wittershagen A.: O*rganometallics*, in press.